Surface Morphological and Electrical Properties of Sputtered Tio$_2$ Thin Films

M.Thaidun[1x], B.Venkata Rao[1], L.Raja Mohan Reddy[1]
Department of Physics,Loyola Degree College (YSRR),Pulivendla,A.P,India.516390

Abstract: - *Titanium dioxide films were formed on quartz and crystalline p-Si (100) substrates by DC reactive magnetron sputtering method. Pure titanium target was sputtered at a constant oxygen partial pressure of 5×10^{-2} Pa, and at different sputtering powers in the range 80 – 200 W. The as-deposited films were annealed in air for 1 hour at 1023 K. The deposited films were characterized by studying the surface morphology by atomic force microscopy (AFM), electrical and dielectric properties from current-voltage and capacitance-voltage measurements. Atomic force micrographs of the films showed that the R_{rms} and R_a increased with the increase of sputter power from 80 to 200 W. The leakage current density was increased by increasing the sputtering power.*
Keyword: - *AFM, DC sputtering technique, Titanium dioxide thin film.*

I.   Introduction

For a long time, TiO$_2$ thin films have got attention in either as an optical material or as a protective layer for very large scale integrated circuits, because of their high refractive index, excellent optical transmittance and good semiconductor properties (3eV gap), high dielectric constant, very good wear resistance, a high chemical resistance against solvents and acids and stability [1-3]. Due to these special properties, TiO$_2$ has become the subject of many investigations for applications in optical coatings, microelectronic devices and protective layers. In the last decade, titanium dioxide has also attracted a great deal of interest due to its photocatalytic behavior [4, 5]. The decomposition of organic compounds on the surface of TiO$_2$ and the reduction of the contact angle between water and the surface of TiO$_2$ under UV irradiation results in self-cleaning and anti-fogging effects [6]. It is well known that titania exhibits three distinct crystalline forms apart from the amorphous form: an orthorhombic one, the brookite and two tetragonal phases, the anatase and the rutile [7, 8]. The occurrence of anatase and rutile phase depends significantly on the method and conditions of deposition as well as the substrate temperature [9]. Each crystalline form is convenient for a different purpose. While rutile is mainly desirable for optical applications, anatase has more efficient photocatalytic properties. Which structure is formed during the fabrication of TiO$_2$ thin films depends on the deposition technique, the deposition parameters and the deposition configuration.

TiO$_2$ films were prepared by various methods, such as chemical vapour deposition, pulsed laser deposition, sol-gel deposition, spray pyrolysis, plasma enhanced chemical vapour deposition and DC/RF magnetron sputtering [10-14]. However for most deposition techniques, a high temperature by use of substrate heating or post-deposition annealing is required for the growth of anatase or rutile phases of TiO$_2$ thin films instated of amorphous films. Compared to other deposition methods, DC Magnetron sputtering technique has significant importance because it enables control of the structure, good adhesion on the substrate of deposited films, high density and homogeneity, composition and properties of TiO$_2$ films by adjusting the deposition conditions. This results in high quality thin films with thickness uniformity over large areas and well controlled stoichiometry.

II.   Experimental

Thin films of TiO$_2$ were deposited on silicon and quartz substrates by sputtering of titanium target under various oxygen partial pressures using the DC modes. The TiO$_2$ films were deposited at oxygen partial pressure of 5×10^{-2} Pa and at a fixed substrate temperature of 303 K and at different sputtering powers in the range 80 – 200 W. The as-deposited films were annealed in air at 750°C for 1 hour. The TiO$_2$ films were deposited on p-type silicon substrate by DC magnetron sputtering and the top electrode of aluminum was deposited using Hind High Vacuum coating unit by vacuum evaporation. The Si wafers were placed in Teflon container. Insoluble organic contaminants in the wafer can be removed by immersing the wafers in the organic clean solution, which is maintained (5:1:1, H$_2$O: H$_2$O$_2$: NH$_4$OH) for 10 minutes. Removed carrier form the organic clean solution and rinse wafer in the deionized water for one minute. Submerge the carrier with wafer in the oxide strip solution (50:1, H$_2$O:HF) for 15 seconds in order to remove silicon dioxide that may be accumulated as a result of organic clean. Then remove carrier from the bath and rinse the wafer in deionized water for one minute. Finally removed the substrates from the substrate carrier contained deionized water and

blown dry with nitrogen. The deposited films were characterized by studying the surface morphology by atomic force microscopy (AFM), electrical and dielectric properties from current-voltage and capacitance-voltage measurements.

III.   Results and Discussion

The dependence of deposition rate of the TiO$_2$ films on the sputtering power is shown in figure 3.1. The deposition rate of the films at a low sputtering power of 50 W was 1.26 nm/min. At low sputtering powers, the target current was low which attributed to the lower argon ion bombardment on the target surface due to lower ion flux results in low sputtering yield. The deposition rate of the films increased from 1.26 to 6.66 nm/ min with the increase of sputter power from 80 to 200 W. At higher sputtering powers, high argon ion flux generally resulted in substantial ion bombardment on the target with high kinetic energy which increased the probability that the impact of incident ions will eject more target atoms [15].

The surface morphological studies of the sputtered TiO$_2$ thin films were carried out by using atomic force microscope. Figure 3.2 shows the atomic force micrographs of the TiO$_2$ films deposited at different sputtering powers. The micrographs showed that the TiO$_2$ films deposited at low sputtering power has a smoother and less dense in structure. At low sputtering powers, the adatoms with low kinetic energy result in negligible surface diffusion. When sputtering power increased to 120 W, the TiO$_2$ films appeared to be continuous with fine sized grains might be due to presence of mixed phase. As the sputtering power increased to 160 W, the grain size of the films increased. The surface diffusion of the adatoms was enhanced with the momentum transfer to the growing surface resulted an increase in the grain size present in the films. The enhancement in crystallinity of the films was achieved at higher sputtering power of 200 W due to larger impact energy of the bombarding particles, which lead to better surface mobility. The higher the sputtering power, the more likely the film formed was of continuous and with higher crystallinity due to sufficient high adatom mobility which improved the surface diffusion. The grain size of the TiO$_2$ films increased as the sputtering power increased. The increase in the grain size was a result of bombardment to the growth surface by more energetic particles with increasing sputtering power was also reported by Song et al. [16].

Figure 3.3 shows the typical leakage current characteristics of the MOS (Al/TiO$_2$/p-Si) structured capacitors for negative and positive applied voltages formed at different sputter powers. For the current – voltage measurements, a step time of 1s and a step voltage of 0.1 V was used. It is seen from the figure that the leakage current density increased with the increase of sputter power. The minimum leakage current density achieved with sputter power of 80 W at a gate bias voltage of 1.5 V was 1.30×10^{-8} A/cm^2 and it was increased to 1.39×10^{-6} A/cm^2 by increasing the sputter power to 200 W. The increase in leakage current density with sputtering power was due to the increase in oxygen defects in the TiO$_2$ films and also increases in the structural defects. Huang et al. [17] was also observed the increase in leakage currents with the increase in sputter power of MgTiO$_3$ films.

Figure 3.4 shows the capacitance-voltage at different frequencies at different frequencies for Al/TiO$_2$/p-Si capacitors formed at different sputtering powers in the range 80 – 200 W and annealed at 1023 K. The capacitance of the TiO$_2$ capacitors was decreased with the increase in frequency. The increase of capacitance of the device at low frequencies depends on the ability of the electron concentration to follow the applied signal. While the decrease of capacitance of the device at high frequencies, the charge at the interface cannot follow an AC signal.

The capacitance–voltage measurements for TiO$_2$ films formed at different sputtering powers were shown in figure 3.5. The experimental characteristics are similar to normal C–V dependence, i.e. accumulation, depletion and inversion could be easily recognized (Fig. 3.5). For negatively biased structure, negative electron charge at the gate is balanced by positive hole charges accumulated near the surface of the semiconductor (p-type). In an ideal MOS system capacitance (C) measured in this accumulation state is equal to oxide capacitance $C_{ox} = 2794 \times 10^{-12}$ F at 80 W. Switching the bias voltage into positive direction makes semiconductor surface depleted from the holes, so that the additional capacitance of space charge layer Cs, is serially connected to C_{ox}. Moreover, the positive gate biasing makes that at low frequency conditions inversion of the conduction type occurs. In the strong inversion conditions, potential changes at the gate are determined by the presence of electrons at the semiconductor metal interface. Thus, the total measured capacitance, similar to the accumulation state, approach to the C_{ox}. The capacitance of TiO$_2$ films was decreased from 2794×10^{-12} to 1309×10^{-12} F with the increase of sputter power from 80 to 200 W [17]. The capacitance of the TiO$_2$ capacitors was increased due to the decrease in the measured thickness of the films with the decrease of sputtering power. From the measured capacitance and physical thickness, the dielectric constant (k) of the TiO$_2$ films can be calculated. The dielectric constant was calculated from the capacitance - voltage curves using the following formula,

$$C = k\varepsilon_o A / t \qquad\qquad (1)$$

Where C is the capacitance, k the dielectric constant of the material, ε_o the permittivity of free space (8.85×10^{-3} fF/µm), A the area of the capacitor, and t the thickness of the dielectric. The dielectric constant of the TiO$_2$

films formed at sputter power of 80 W was 10 and it increased to 35 with the increase of sputtering power to 200 W. Figure 3.6 shows the dependence of dielectric constant on sputter power. The dielectric constant of the films increased with the increase of sputter power. These annealed films at different sputter powers leads to decrease of structural defects, and change the phase transformation from anatase to rutile phase, hence enhance in the dielectric constant of the TiO_2 films.
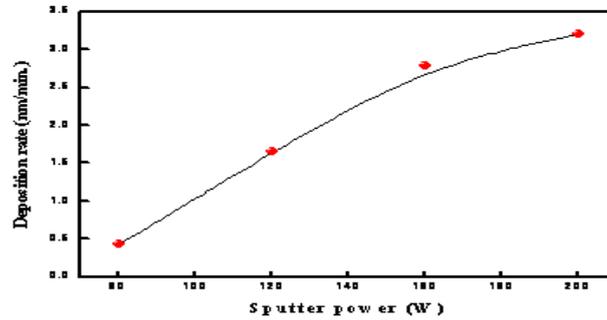
IV.   FIGURES

Fig.3.1. Variation of deposition rate with sputter power of TiO_2 films.

Fig.3.2. Atomic force micrographs of TiO_2 films formed at: (a) 80, (b) 120, (c) 160 and (d) 200 W
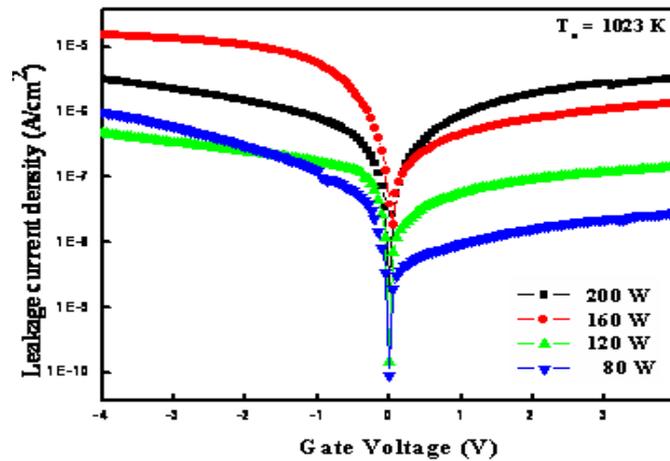
Fig. 3.3. I-V characteristics of TiO₂ films formed at different sputter powers.
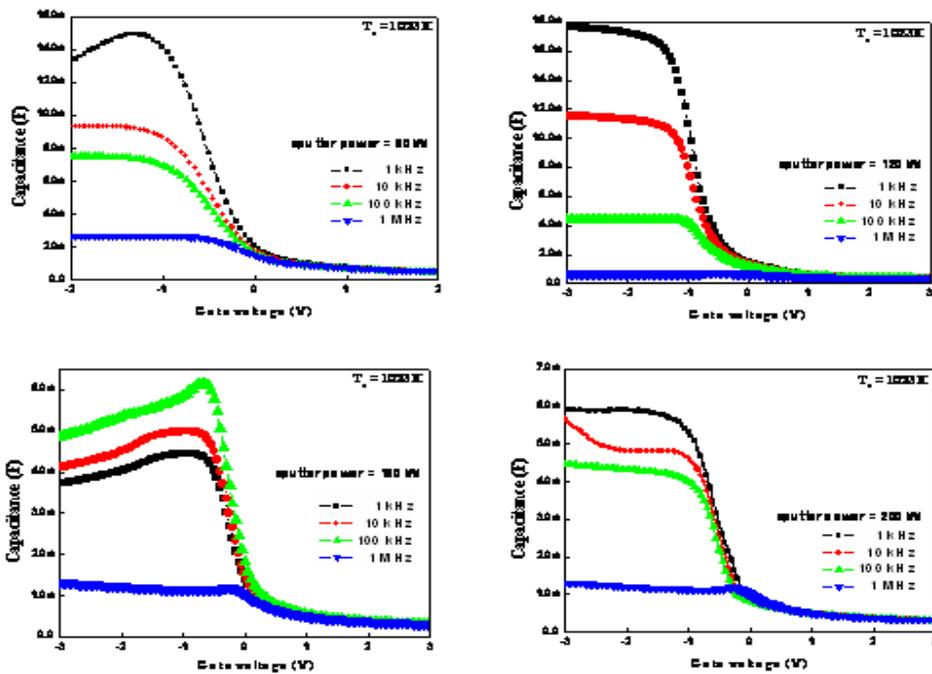

Fig. 3.4 Capacitance – Voltage curves of Al/TiO₂/p-Si capacitors at different Frequencies.
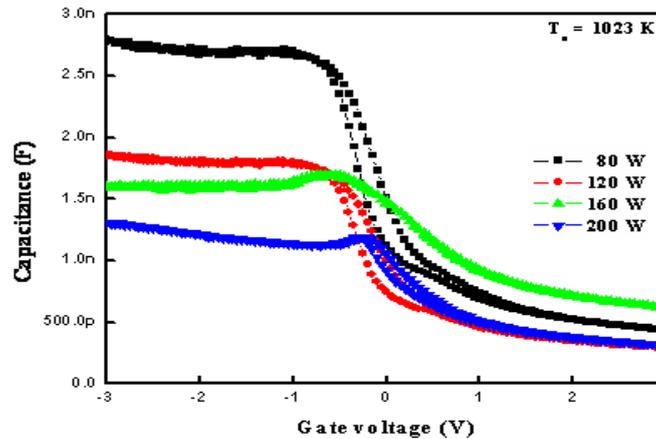

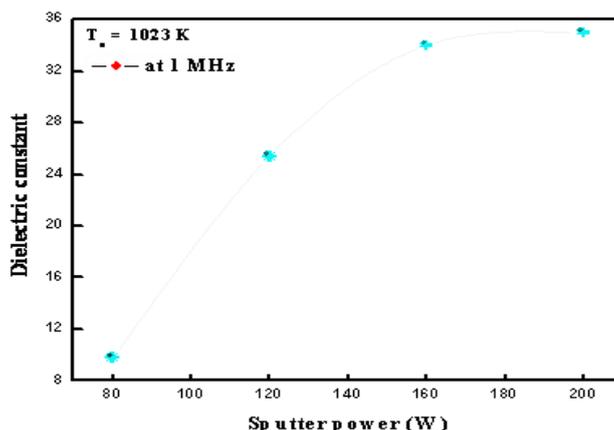Fig. 3.5 Capacitance – Voltage curves (at 1 MHz) of Al/TiO₂/p-Si capacitors

Fig. 3.6 Variation of dielectric constant with sputter powers

V.   Conclusion

In conclusion, TiO$_2$ films formed at sputter power of 80 W and annealed at 1023 K were polycrystalline in nature with anatase phase, the grain size of the TiO$_2$ films increased as the sputtering power increased. The leakage current density and dielectric constant was increased by increasing the sputtering power.

References

[1]   Y. Leprince-Wang, D. Souche, K. Yu-Zhang, S. Fisson, G. Vuye and J. Rivory, Thin Solid Films, **359** (2000) 171.
[2]   P. Zeman and S. Takabayashi, Surface and Coatings Technology, **93** (2002) 153.
[3]   L. Miao, P. Jin, K. Kaneko, A. Terai, N. Nabatova-Gabain and S. Tanemura, Applied Surface Science, **255** (2003) 212.
[5]   R. Wang, K. Hashimoto, A. Fujishima, M. Chikuni, E. Kojima, A. Kitamura, M.Shimohigoshi and T. Watanabe, Nature, 388 (1997) 431.
[6]   T. Watanabe, A. Nakajima, R. Wang, M. Minabe, S. Koizumi, A. Fujishima and K. Hashimoto, Thin Solid Films, 351 (1999) 260.
[7]   K. Takagi, T. Makimoto, H. Hiraiwa and T. Negishi, J. Vac. Sci. Technol., A 19(6) (2001) 2931.
[8]   S. Ben Amor, G. Baud, J. P. Besse and M. Jacquet, Materials Science and Engineering, B47 (1997) 110.
[9]   J. Szczyrbowski, G. Bräuer, M. Ruske, J. Bartella, J. Schroeder and A. Zmelty,   Surface and Coatings Technology, 112 (1999) 261.
[10]   N. Martin, C. Rousselot, D. Rondot, F. Palmino and R. Mercier, Thin Solid Films,   300 (1997) 113.
[11]   M. Takeuchi, N. Yamasaki, K. Tsujimaru, Chem. Lett., 35 (2006) 904.
[12]   A. Verma, A.G. Joshi, A.K.Bakshi, S.M. Shivaprasad and S.A. Agnihotry, Appl. Surf. Sci., 252 (2006) 5131.
[13]   I.Turkevych, Y. Pihosh, M. Goto, A.Kasahara, M. Tosa, S. kato, K. Takehana, T. Takamasu, G. Kido and N. Koguchi, Thin Solid Films, 516 (2007) 2387.
[14]   M. Vishwas, S.K. Sharma, K. Narshimha Reao, S. Mohan,K.V.A. Gowda and R.P.S. Chakradhar, Spectrochim. Acta, Part A 74 (2009) 839.
[15]   Nirupama and S. Uthanna, J. Mater. Sci.: Mater. Electron., 21 (2010) 45.
[16]   Y.S. Song, J.K. Park, T.W. Kin and C.W. Chung, Thin Solid Films, 467 (2004) 120.
[17]   C.L. Huang and Y.B. Chen, J.Cryst. Growth, 285 (2005) 586.